# Substrate-Specific Conformational Regulation of the Receptor Tyrosine Kinase VEGFR2 Catalytic Domain

James Solowiej, Jeffrey H. Chen, Helen Y. Zou, Stephan K. Grant, and Brion W. Murray*

Oncology Research Unit, Pfizer Worldwide Research and Development, 10777 Science Center Drive, San Diego, California 92121, United States

ABSTRACT: The contributions of the phosphoacceptor and the catalytic domain context to protein kinase biology and inhibitor potency are routinely overlooked, which can lead to mischaracterization of inhibitor and receptor functions. The receptor tyrosine kinase vascular endothelial growth factor receptor-2 (VEGFR2) is studied as a model system using a series of phosphoacceptor substrates (k_{cat}/K_m 684–116,000 $M^{-1} s^{-1}$) to assess effects on catalysis and inhibitor binding. ATP-competitive inhibitor potency toward the VEGFR2 catalytic domain (VEGFR2-CD) varies with different phosphoacceptor substrates, which is unexpected because the phosphoacceptors do not affect $K_{m,ATP}$ values. Indazole-based inhibitors are up to 60-fold more potent with two substrates (gastrin, minigastrin) relative to the others. Thus there is a component of uncompetitive inhibition because a specific phosphoacceptor enhances potency but is not strictly required. This substrate-specific inhibitory potency enhancement correlates with phosphoacceptor active site saturation and is not observed with other related kinases. The effect is confined to a specific catalytic domain conformation because autophosphorylation eliminates the potency enhancement as does the addition of the juxtamembrane domain (20 amino acids). Indazole inhibitor structure–activity analysis reveals that the magnitude of potency enhancement correlates with the size of the substituent that binds in a regulatory region of the active site. VEGFR drugs profiled with VEGFR2-CD using minigastrin have potency well-correlated with inhibition of full-length, cellular VEGFR2 autophosphorylation, an indication that the minigastrin-induced conformation is biologically relevant. These findings raise the possibility that inhibitors directed toward a common target can have different biological effects based on the kinase–substrate complexes present in different cellular contexts.
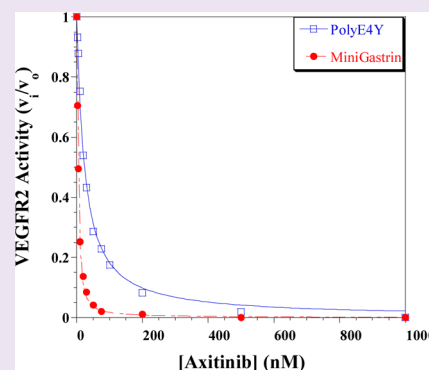
Receptor tyrosine kinases (RTKs) have central roles in cellular signaling for normal physiology as well as pathological processes, which makes them frequent targets for therapeutic intervention.[1] A prototypical RTK is the vascular endothelial growth factor receptor-2 (VEGFR2, KDR, FLK-1), which is a type III receptor tyrosine kinase with seven related family members: VEGFR1 (FLT1) and VEGFR3 (FLT4), FLT3, cKit, PDGFRα, PDGFRβ, and CSF1R/FMS.[2,3] In order to affect signal transduction, membrane-bound VEGFR2 catalyzes an autophosphorylation reaction that enhances enzymatic activity and creates docking sites for recruitment and phosphorylation of other signaling proteins.[4–6] VEGFR2 is composed of multiple domains that perform distinct biological functions: an extracellular ligand binding domain with seven immunoglobulin-like motifs, a single transmembrane domain, a juxtamembrane domain (JM), a catalytic domain (CD) split by a kinase insert domain, and a C-terminal docking domain.[7,8] The catalytic domain shares the overall structure common to all protein kinases composed of two subdomains (N- and C-terminal) with catalysis occurring at the interface in the typical random ordered kinetic mechanism.[1] This complex system of domains and subdomains is well-integrated to yield a signaling protein with strictly controlled biological function.

VEGFR2 regulation is affected by a diverse array of mechanisms: synthesis, limited proteolysis, degradation, post-translational modification, conformational modulation, and subcellular localization.[9] Extracellular VEGF ligand induces autophosphorylation of the intracellular catalytic domain's C-terminal activation loop residues. This well-characterized post-translational mechanism affects catalytic activity, realigning critical catalytic residues and the overall catalytic domain conformation.[1,7,10–12] The VEGFR2 C-terminal docking domain autophosphorylation primarily affects signaling protein recruitment and not catalysis.[9,12–15] More recently, autophosphorylation of a JM domain tyrosine residue has been shown to affect its interactions with both N- and C-terminal lobes of the catalytic domain, altering the active site topography and conformation dynamics.[10] This led to a model in which the JM domain spans the two catalytic domain lobes to regulate the conformations, conceptually a "thermodynamic clasp" that also affects inhibitor affinity.[10] Subsequently, the structural underpinnings of these interactions were crystallographically defined.[16] Recent studies show that VEGFR2 is regulated through subcellular localization with alternative proteolytically truncated forms that continue to function inside the cell to activate a set of signaling proteins different than those activated

by membrane-bound VEGFR2.[9,17] Taken in the whole, VEGFR2 is tightly regulated through a diverse array of mechanisms and has context-specific biological functions.

Receptor tyrosine kinases have been successfully targeted for therapeutic intervention by small molecule kinase inhibitors, with many drugs either successfully having completed clinical trials or in late-stage clinical studies.[1] To date, at least 16 distinct small molecule VEGFR2 drugs have entered advanced clinical trials with five achieving FDA approval (axitinib, sunitinib, sorafenib, pazopanib, vandetanib).[1] Small molecule VEGFR2-directed drugs, as for most agents that target RTKs, inhibit the catalytic domain function in an ATP-competitive mode yet bind to different catalytic domain conformations.[1,8,16,18,19] Recent studies have shown that the juxtamembrane domain (JM) can alter inhibitor binding to the catalytic domain with a subset of drugs characterized for binding energetics and molecular interactions with a VEGFR2-CD/JM protein to reveal three distinct binding modes for non-active conformation-directed drugs: JM displacing inhibitors (Type II), JM_{in}-complementary inhibitors (Type IVa), and JM_{in}-compatible inhibitors (Type IVb).[10,16] These conformation-specific inhibitor interactions place a premium on identifying factors that affect the catalytic domain conformation.

In this study we identify substrates that specifically alter the VEGFR catalytic domain active site topography affecting inhibitor interactions that are well-correlated with endogenous, full-length VEGFR2 cellular responses. These findings allow the model of catalytic domain regulation by the JM domain, the "thermodynamic clasp",[10] to be extended to include phosphoacceptors with interactions to both N- and C-terminal lobes. Thus, elements that simultaneously bind both catalytic domain lobes can alter the equilibrium between populations of catalytic domain conformations.

■ RESULTS AND DISCUSSION

Identification of Efficient VEGFR2 Substrates. Many types of phosphoacceptor substrates are routinely used to characterize enzymatic activity and inhibitor interactions. We chose a range of phosphoacceptor types to study in order to understand the extent of the phosphoacceptor involvement in inhibitor binding. Poly(Glu₄Tyr) is included because it is the most common RTK substrate and has both protein and peptide attributes: average molecular weight of 20 kDa, wide range of peptide sizes, and a simple amino acid sequence. Gastrin peptides (gastrin, progastrin$_{55-71}$, G17; minigastrin, progastrin$_{59-71}$) have structural similarities to poly(Glu₄Tyr) but are a single chemical entity. Unlike poly(Glu₄Tyr), gastrins have a single tyrosine residue and thus can have only a single phosphotransfer reaction for each binding event eliminating the possibility of processivity. In the context of a catalytic domain, activation loops are known to have a high degree of conformational freedom, so activation loop peptides represent physiologically relevant substrates (KDRtide, METtide). General protein substrates are routinely used in kinase assays, so a protein substrate was identified and characterized (dephosphorylated α-casein). Evaluation of dephosphorylated α-casein revealed that it is a less efficient substrate than the tested peptides, so focus was shifted to peptide substrates (Table 1). The peptide K_m values varied over 10-fold as did the k_{cat} values with nonphosphorylated VEGFR2-CD. As such, the efficiencies (k_{cat}/K_m) of the phosphoacceptors varied from 684 to 116,000 M^{-1} s^{-1} (Table 1). Gastrin peptides are the most efficient substrates with k_{cat}/K_m values from 82,400 to 116,000

Table 1. Kinetic Evaluation of Nonphosphorylated VEGFR2-CD Phosphoacceptor Substrates at a Saturating Concentration of ATP

	$K_{m,peptide}$ (mM)	k_{cat} (s^{-1})	k_{cat}/K_m (M^{-1} s^{-1})
poly(Glu₄Tyr)[a]	4.0 ± 0.2	26 ± 1	6,700 ± 400
minigastrin	0.52 ± 0.05	43 ± 1	82,000 ± 2000
gastrin[a]	0.31 ± 0.01	36 ± 1	120,000 ± 4000
KDRtide	4.6 ± 2.9	3.2 ± 1.2	680 ± 420
METtide	2.2 ± 0.1	24 ± 1	10,000 ± 1100
MET2	4.1 ± 1.6	11 ± 4	2,800 ± 1400
dephosphorylated αCasein protein	0.13 ± 0.02	0.80 ± 0.08	6,400 ± 1900

[a]Previously reported.[10]

M^{-1} s^{-1} and had the greatest k_{cat} values (36–43 s^{-1}). The effects of the phosphoacceptors on $K_{m,ATP}$ values were evaluated at a high peptide concentration. No significant differences are observed in the ATP K_m values: 0.776 ± 0.025 mM poly(Glu₄Tyr), 0.789 ± 0.045 mM minigastrin (MG), and 0.757 ± 0.057 mM METtide. Autophosphorylation of VEGFR2-CD did not profoundly change the kinetic values for phosphorylation of MG ($K_{m,ATP}$ = 0.153 ± 0.020 mM, $K_{m,MG}$ = 0.142 ± 0.014 mM, k_{cat} = 20.0 ± 0.9 s^{-1}). From this basic kinetic analysis, a range of phosphoacceptor substrates with diverse properties was identified.

Characterizing the VEGFR2 Active Site with Small Molecule Inhibitors. Since the VEGFR2 kinase inhibitors are ATP-competitive, not phosphoacceptor-competitive, there was no expectation for a contribution of the phosphoacceptor to inhibitor potency. However, small molecule inhibitors can be more sensitive probes of the active site topography than substrates, and as such, axitinib potency was studied as a function of phosphoacceptor type (Table 2). Interestingly,

Table 2. Evaluation of the Inhibition of Axitinib As a Function of Kinase and Phosphoacceptor[a]

kinase	phosphoacceptor	axitinib K_i (nM)	fold change
VEGFR2	poly(Glu₄Tyr)	1.10 ± 0.18	1
	KDRtide	0.88 ± 0.23	1
	METtide	0.69 ± 0.12	2
	minigastrin	0.052 ± 0.14	21
	gastrin	0.059 ± 0.018	19
VEGFR1	poly(Glu₄Tyr)	2.9 ± 0.3	1
	minigastrin	0.44 ± 0.09	7
FGFR1	poly(Glu₄Tyr)	34 ± 2	1
	minigastrin	32 ± 2	1
PDGFRβ	Poly(Glu₄Tyr)	1.4 ± 0.2	1
	minigastrin	2.6 ± 0.4	0.5

[a]The phosphoacceptor concentrations were fixed: poly(Glu₄Tyr) was 7.5 mM, and the peptide substrates were 0.5 mM concentrations. All kinases were tested as nonphosphorylated catalytic domain proteins with no time-dependent inhibition observed. The fold change in potency is calculated relative to the axitinib K_i determined using poly(Glu₄Tyr).

axitinib is found to be 21-fold more potent at inhibiting VEGFR2-CD with MG as the substrate (CD+MG) relative to when poly(Glu₄Tyr) is used (CD+PGT). This finding is surprising because the gastrin peptides are structurally similar to poly(Glu₄,Tyr) with the phosphorylated tyrosine residue flanked by a series of glutamate residues. In contrast, the

Table 3. Evaluation of the Structure–Function Relationship of Indazole-Based Inhibitor Potency on Nonphosphorylated VEGFR2 as a Function of Protein Construct and Substrate[a]

	R_2	X	R_1	VEGFR2-CD Ki (pM)			VEGFR2-CD/JM K_i (pM)		Cell IC$_{50}$ (pM)
				poly(Glu$_4$Tyr)	Minigastrin	Ratio poly(Glu$_4$Tyr) vs MG	poly(Glu$_4$Tyr)	Minigastrin	VEGF-stimulated HUVEC Survival
Axitinib	(pyridinyl-vinyl)	S	—CH$_3$	1100 ± 55	52 ± 4	21	28 ± 3	65 ± 29	180 ± 80
1	(pyridinyl-vinyl)	S	propyl	303 ± 37	20 ± 2	15	18 ± 4	150 ± 26	210
2	(pyridinyl-vinyl)	S	cyclobutyl	1130 ± 71	130 ± 13	9	140 ± 20	690 ± 120	620
3	(pyridinyl-vinyl)	NH	cyclopropyl	370 ± 39	88 ± 15	4	160 ± 21	430 ± 69	490
4	(pyridinyl-vinyl)	S	allyl (CH$_2$)	350 ± 13	64 ± 8	5	40 ± 5	88 ± 14	280
5	(pyridinyl-vinyl)	S	propargyl (≡CH)	210 ± 17	120 ± 28	2	33 ± 6	230 ± 37	110
AG-013958	(pyridinyl-vinyl)	NH	(dimethyl-pyrazolyl)	300 ± 48	270 ± 36	1	35 ± 5	110 ± 20	310 ± 100
6	(H$_3$C amide)	S	—CH$_3$	15000 ± 480	260 ± 15	58	630 ± 62	530 ± 29	6600
7	(azaindolyl)	S	—CH$_3$	1100 ± 20	27 ± 4	40	50 ± 4	56 ± 2	100

[a]Poly(Glu$_4$Tyr) was held constant at 20 mM, and 0.5 mM minigastrin was used. Inhibition of VEGF-dependent cell survival in HUVEC was measured. Axitinib findings using poly(Glu$_4$Tyr) have been published previously.[10]

affinities of axitinib using either activation loop peptides from VEGFR2 and cMet are similar to potencies derived using poly(Glu$_4$Tyr) (Table 2). The enhanced axitinib affinity observed for CD+MG is well-correlated with the affinity derived with the nonphosphorylated VEGFR2 construct containing both catalytic and juxtamembrane domains (VEGFR2-CD/JM), which has been recently shown to better predict cellular and clinical effects[10,16] (Table 3). Inhibition of VEGFR2-CD/JM is less dependent on the phosphoacceptor, as potency derived using either poly(Glu$_4$Tyr) or MG varies very little (<3-fold). The specificity of the axitinib potency enhancement was studied by profiling other VEGFR2 family members (Table 2, Figure 1). Axitinib potency toward VEGFR1 with MG is enhanced to a lesser degree. With the other highly related receptor tyrosine kinases (FGFR1, PDGFRβ) there is no measurable substrate-specific MG effect. From this analysis, axitinib exhibits a specific, partially uncompetitive inhibition because VEGFR2 inhibition is enhanced but not strictly dependent on MG substrate binding.

The factors that influence the catalytic domain conformation were characterized. Inhibition of autophosphorylated VEGFR2 is profiled because autophosphorylation alters the catalytic domain to an active conformation.[10] As the indazole-based inhibitors are designed to bind to a non-active conformation of VEGFR2, the effect of autophosphorylation on the substrate-specific potency enhancement could provide insight on the conformational specificity of the interaction. As expected, the indazole inhibitors are less potent toward autophosphorylated VEGFR2 when poly(Glu$_4$Tyr) is used as the phosphoacceptor: phospho-VEGFR2-CD (axitinib K_i = 7200 ± 900 pM; 7 K_i = 5600 ± 440 pM); phospho-VEGFR2-CD/JM (axitinib K_i = 1200 ± 130 pM; 7 K_i = 2000 ± 240 pM) (see Table 3 for comparisons). This finding also shows that inhibitor affinity

enhancement achieved by the addition of the JM domain is eliminated by autophosphorylation. Autophosphorylation of VEGFR2-CD also eliminates the potency enhancement of axitinib observed when MG is used as the phosphoacceptor substrate (K_i = 1300 ± 120 pM), which is 26-fold less potent than inhibition of nonphosphorylated VEGFR2-CD using MG (CD+MG) (Table 2). Potential contributions of the full-length VEGFR2 protein or the cellular environment to the binding conformation of VEGFR2 catalytic domain were also evaluated. The CD+MG inhibition potency is well-correlated with the cellular potency measuring inhibition of VEGF-dependent HUVEC survival (Table 3) and VEGF-stimulated full-length VEGFR2 autophosphorylation in PAE cells. (Table 4). These findings are consistent with a hypothesis that the substrate-dependent potency enhancements are based on specific interactions with VEGFR proteins to select a physiologically relevant catalytic domain conformation.

To gain a deeper understanding of the substrate-dependent potency effect on the VEGFR2-CD active site, inhibitor affinity was determined for a matched series of indazole-based inhibitors to establish a structure–activity relationship (Table 3). The indazole core binds directly to the hinge region of the active site with two vectors at the indazole 3- and 6-postions.[10,16] The 6-position aligns substituents toward the regulatory pocket (back pocket) that is available in the non-active catalytic domain conformation.[16,24] When the indazole 6-position is varied with a constant 3-position substituent (Table 3, axitinib to AG-013958), the observed CD+MG potency enhancement varies with the substituent size. As the 6-substituent extends deeper, the inhibitor binding mode can be expected to switch to a JM-displacing binding mode (Type II). Substituents at indazole 3-position at constant 6-position substitution affect an additional 2−4-fold enhancement in
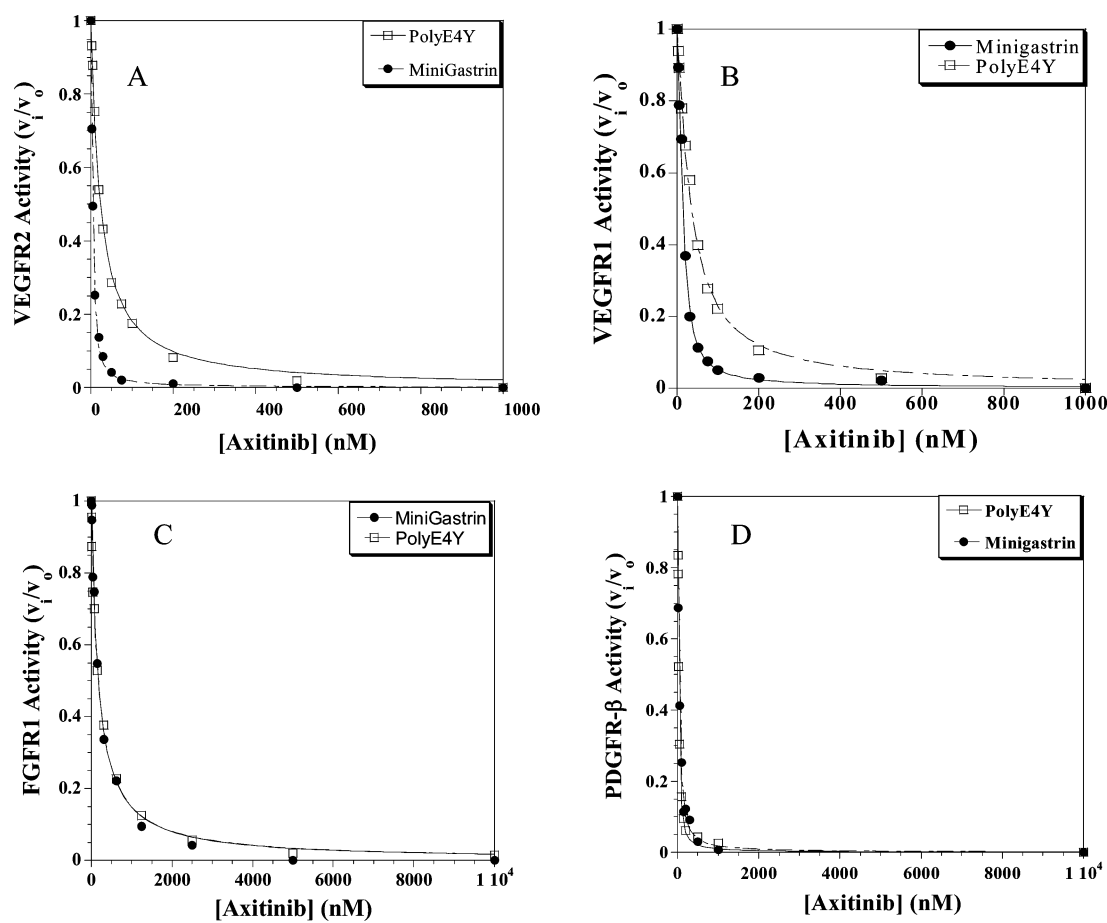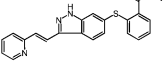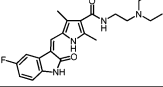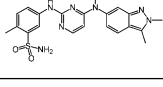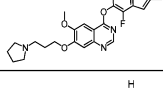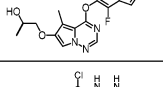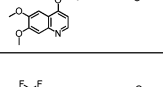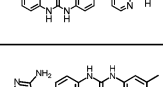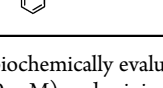
Figure 1. Effect of the phosphoacceptor substrate on axitinib inhibitory potency for related receptor tyrosine kinases. Potency of axitinib was determined with either 0.5 mM minigastrin (●) and 20 mM poly(Glu$_4$,Tyr) (□) for the following kinases: (A) VEGFR2, (B) VEGFR1, (C) FGFR1, and (D) PDGFRβ. The fitted data are in Table 2.

affinity with MG as the VEGFR2-CD substrate: **6, 7**, axitinib. The biochemical SAR using nonphosphorylated VEGFR2-CD/JM is correlated with affinity determined with CD+MG (R^2 = 0.60) compared to CD+PGT (R^2 = 0.33) (Table 3). These results are expected because the inhibitors span Type II and Type IV (JM-compatible) binding modes. Inhibitor potency enhancements are determined as a function of MG concentration. Two highly related indazole inhibitors are selected that had either a large substrate-specific potency enhancement (axitinib) or no effect (AG-13958) due to the size of the back pocket binding substituent.[24] For axitinib, but not the structurally related inhibitor AG-13958, the change in inhibitory potency correlated with the degree of MG substrate saturation of VEGFR2 (Figure 2A). The half-maximal MG effect on the axitinib affinity (K_i) value is at 0.540 ± 0.167 mM MG, which is well-correlated with the MG K_m value determined in the same experiment, 0.412 ± 0.054 mM. As such, the substrate-specific inhibition enhancement can be saturated. In addition, at a saturating MG concentration, the maximal axitinib K_i value was calculated to be 16 ± 1 pM, which is equivalent to the potency toward VEGFR2-CD/JM.[10,16] Next, the impact of MG on the inhibitor mechanism of action is studied to determine if the enhanced potency arises from an altered mechanism. Using tight-binding kinetic inhibitor analysis, inhibitors with and without a MG-specific potency enhancement (axitinib, AG-13958) exhibit linear relationships between apparent affinity (K_i^{app}) and ATP concentration with

MG as the phosphoacceptor which is consistent with an ATP-competitive mechanism of action (Figure 2B).

The VEGFR2 substrate-dependent effect on inhibitor affinity was explored with a set of chemically diverse inhibitors composed of advanced investigational and FDA-approved VEGFR drugs that are all ATP-competitive inhibitors but known to bind to different catalytic domain conformations (Table 4).[1,16,25] The drugs were profiled with VEGFR2-CD and commercially available GST-VEGFR2 (Table 4). The VEGFR2 drugs are up to 20-fold more potent toward inhibiting CD+MG relative to CD+PGT. Rank order biochemical affinities using CD+MG to assess inhibitor activity are better correlated with inhibitor potency of VEGF-induced cellular autophosphorylation (R^2 = 0.57) than with CD+PGT (R^2 = 0.26) (Table 4). The GST-VEGFR2 protein can coarsely detect rank-order potencies for inhibition of cellular VEGFR2 autophosphorylation. For predicting absolute cellular potency, the K_i values determined using purified kinases are expected to be greater than in a whole cell assay because of the additional complexities affecting potency (e.g., permeability, efflux, protein binding). The GST-VEGFR2-derived potency was weaker than the cell potency for 7 of the 8 tested drugs. The CD+PGT potency was greater with 3 of 8 drugs more potent in the biochemical assay. For CD+MG, the measured drug potency was greater than cellular potency for 6 of 8 drugs. As such, MG induces a specific, physiologically relevant catalytic domain conformation.

Table 4. VEGFR2 Drug Potency As a Function of Phosphoacceptor and Catalytic Domain Context[a]

Drug	Structure	Non-phosphorylated VEGFR2-CD		GST-VEGFR2	PAE/KDR Cells	Inhibitor Binding Type	HUVEC
		Poly(Glu$_4$Tyr)	MG	CSKtide	Autophosphorylation		VEGF-mediated survival
		K_i (pM)	K_i (pM)	K_i (pM)	IC$_{50}$(pM)		IC$_{50}$ (pM)
Axitinib		1100 ± 60	52 ± 4	1200 ± 100	41 ± 33	IVa	180 ± 80
Sunitinib		60000 ± 900	15000 ± 600	15000 ± 800	3400 ± 2800	I/IVb	14000 ± 4300
Pazopanib		8200 ± 100	300 ± 20	2900 ± 200	580 ± 400	IVb	12000 ± 7200
Cediranib		8100 ± 200	3400 ± 80	1300 ± 100	380 ± 250	IVb	7400 ± 5500
Brivanib		44000 ± 900	23000 ± 700	12000 ± 1100	28000 ± 7600	IVb	52000 ± 19000
Tivozanib*		200 ± 7	13 ± 1	480 ± 50	140 ± 50	II	460 ± 210
Sorafenib*		580 ± 50	330 ± 20	8600 ± 900	5500 ± 1100	II	25000 ± 11000
Linifanib*		640 ± 50	670 ± 20	11000 ± 700	1600 ± 1600	II	760 ± 280

[a]The drugs were biochemically evaluated using nonphosphorylated VEGFR2-CD or an uncharacterized phosphorylation state of GST-VEGFR2 with poly(Glu$_4$Tyr) (20 mM) and minigastrin (0.5 mM) as the phosphoacceptors. Full-length VEGFR2 autophosphorylation was quantitated by ELISA analysis of lysates from VEGFR2-expressing engineered PAE cells. Inhibitor binding modes: active conformation (Type I); non-active conformation: JM displacer (Type II), JM$_{in}$-complementary (Type IVa), and JM$_{in}$-compatible (Type IVb).[16]
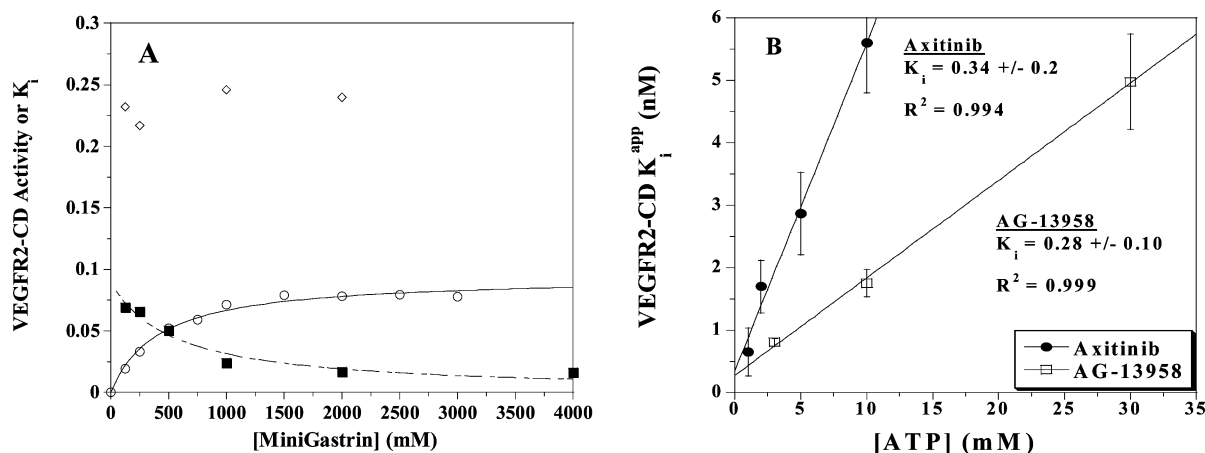

Figure 2. Evaluation of the minigastrin substrate-specific effect on the mechanism of inhibition. (A) The degree of inhibition enhancement for axitinib K_i values (■) was correlated with the amount of VEGFR2 substrate saturation by minigastrin (○) at a fixed ATP concentration (3 mM). The half-maximal effects were similar in magnitude: $K_{m,MG} = 0.412 \pm 0.054$ mM and the half-maximal effect on K_i values, $K_{1/2\ max} = 0.540 \pm 0.167$. Maximal axitinib potency was calculated to have a $K_i = 16 \pm 1$ pM The related indazole inhibitor AG-13958 (◇) was used as a control in which there was no minigastrin-dependent effect on potency. (B) The inhibitors axitinib (●) and AG-13958 (□) were ATP-competitive by tight-binding kinetic analysis when minigastrin (0.5 mM) was used as a substrate. This finding is consistent with a specific effect on the binding topography and not an alteration in the overall architecture of the catalytic domain.

Analysis of Phosphoacceptor Substrate Recognition by VEGFR2.

The investigation of different phosphoacceptor substrates led to unexpected findings including insights into substrate recognition. Although gastrin peptides are structurally

related to poly(Glu$_4$Tyr) with multiple consecutive glutamate residues adjacent to a single tyrosine in the middle of the sequence, they are better substrates than poly(Glu$_4$Tyr) and activation loop peptides. Activation loops are commonly thought to be disordered structural elements that can be mimicked by peptides but lack in the high local concentration that comes with its incorporation into the catalytic domain structure. Interestingly, the activation loop peptide derived from cMet is a much more efficient VEGFR2 substrate compared to the VEGFR2 activation loop peptide. This indicates that activation loop recognition in the autophosphorylation reaction may be more complex than a simple, bimolecular interaction. Minigastrin may also have complex interactions with the catalytic domain. Protein kinase phosphoacceptor substrates are commonly thought to bind in a C-terminal subdomain groove but in fact engage N-terminal subdomain residues directly and indirectly through ATP interactions.[1,26,27] The degree of N-terminal engagement may vary as a function of phosphoacceptor. For MG, the tyrosine residue must bind in the cleft between the two lobes to be phosphorylated and is in the middle of the MG peptide. One peptide terminus has Asp-Phe residues that could bind in the DFG activation loop binding site. As such, N- and C-terminal lobe interactions with minigastrin are possible, which could enhance the efficiency of the tyrosine alignment for the phosphotransfer reaction or alter the catalytic domain to favor the active conformation. Other possible models for the catalytic efficiency exist, such as nonspecific conformation-altering interactions. In normal physiology, gastrin peptides are produced in the G cells of the gastric antrum and control the release of acid within the stomach.[28] However, many studies show that a wide array of tumors aberrantly produce gastrin through *de novo* activation of the gastrin gene following early mutational events.[28−32] Gastrin has well-documented functional roles in cancer that include angiogenesis, apoptosis, and proliferation.[28−32] For example, gastrin has been shown to induce HUVEC tubule formation and induce VEGF production.[32] Studies of the molecular underpinnings of gastrin function in cancer show gastrin-mediated regulation of key signaling molecules: c-Jun, c-Myc, COX2, β-catenin, Erk, and Src.[32] Phosphorylation of gastrin by RTKs has been documented.[33] Taken together, gastrins are excellent VEGFR2 substrates.

Substrate-Specific Effects on the VEGFR2 Active Site Topography. Enzyme kinetic parameters are a coarse measure of the active site limited to interactions that affect catalysis. More sensitive probes of the active site topography are usually active site directed inhibitors. For VEGFR2, inhibitor potency is not expected to vary as a function of the phosphoacceptor peptide characteristics because the $K_{m,ATP}$ values are essentially invariant on the peptide characteristics, and the studied inhibitors are ATP-competitive. Nonetheless, a large phosphoacceptor-specific enhancement in inhibitor potency is observed with gastrin peptides. By many measures, the substrate-dependent inhibition enhancement is a specific phenomenon. It is not observed for other related receptor protein kinases and correlates with the degree of active site substrate saturation. The substrate-dependent effect targets a subset of catalytic domain conformations because autophosphorylation of VEGFR2 ablates the substrate-specific potency enhancements as well as the addition of the JM domain (20 amino acid residues). In addition, at a saturating MG concentration, the axitinib affinity using VEGFR2-CD is nearly identical to the reported affinity using VEGFR2-CD/JM.[10,16] These findings suggest that MG alters the conformation of the non-active VEGFR2 catalytic domain in a manner that may be analogous to the juxtamembrane. This is important because gastrin peptides are routinely used in RTK assays (including VEGFR2) to assess inhibitor potency without the knowledge of its potential biochemical implications.[34−36]

The substrate-dependent modulation of the active site has an additional precedent. Substrate-induced kinase conformational changes can be found with metabolic kinases in which phosphoacceptors are known to alter the catalytic domain to affect catalytic properties. Seminal studies of hexokinase served as a foundation for the induced-fit theory of enzyme catalysis.[37] An intriguing consequence of substrate-specific potency for protein kinase drugs is that there may be unique cellular context-specific effects on signal transduction based on the substrates present; different VEGFR2 drugs may have different cellular effects based on the potency of protein kinase−substrate complexes present.

Inhibitor Binding Modes Place Constraints on Relevant Biochemical Potency. The biochemical analysis of a larger panel of inhibitors and drugs shows that CD+MG predicts both inhibitor rank order and physiologically relevant inhibitor potencies. Recent studies defined the energetic and structural effects for drugs binding to the VEGFR2 catalytic domain to define new inhibitor binding modes[10,16] that can be used to add a structural context for the observed inhibitor potencies toward CD+MG and CD+PGT. Sunitinib extends only a few atoms beyond the ATP site and is capable of binding the active conformation[18] yet has been recently shown to bind to a non-active conformation.[16,38] For sunitinib, the non-phosphorylated VEGFR2 proteins (CD+MG, CD+PGT) under-represent sunitinib potency relative to full-length VEGFR2 in cells. Potency of Type II drugs (tivozanib, sorafenib, linifanib) using CD+MG is greater than in cells, possibly because the inhibition does not require the energetic penalty of JM domain displacement. Inhibition of CD+PGT has a tighter correlation to cell potency for Type II inhibitors, presumably because the inhibitors have to pay an energetic penalty for altering/inducing a specific conformation. The Type IVb JM$_{in}$-compatible drugs (pazopanib, cediranib, brivanib) and the Type IVa JM$_{in}$-complementary drug (axitinib) exhibited inhibition of CD+MG that is tightly correlated with the inhibition of cellular autophosphorylation. For CD+PGT, it under-represented cellular potency for Type IV inhibitors presumably because the appropriate catalytic domain conformation is not available or is in a minor population. Inhibition of GST-VEGFR2-mediated peptide (KKKEEIYFFF) phosphorylation by VEGFR2 drugs shows only a coarse trend to cellular potency even though the assay is a high-quality, mobility-shift assay.[39] This could be due to the GST affinity tag, the peptide substrate, or the simple kinetic analysis (no accounting for tight-binding phenomena). From the study of this diverse panel of drugs that span the known inhibitor binding modes, it is apparent that the catalytic domain environment (substrate, protein context) is critical for the determination of meaningful inhibitor binding energetics to facilitate interpretation of biological effects in more complex systems.

Conclusions. Substrate-specific inhibitor potency enhancement extends the concept of conformational regulation of the protein kinase catalytic domain by entities that span the N- and C-terminal subdomains from the kinase itself (e.g., JM domain) to phosphoacceptor substrates. As such, there is the possibility

for differential biological effects of kinase drugs targeting different topographies of the same kinases dependent on the substrates present in the affected cell.

■ METHODS

Human minigastrin (LEEEEEAYGWMDF) and gastrin (QGPW-LEEEEEAYGWMDF) were purchased (Bachem). Poly(Glu$_4$Tyr) was from Sigma Chemical Company. VEGFR2(786−805) peptide was synthesized and purified to 98% purity (CPC Scientific). Activation loop peptides were synthesized to >90% purity (Pfizer, La Jolla): VEGFR2 (Ac-LARDIYKDPDYVR-K KDR-tide); cMet (Ac-LARD-MYDKEYYSK, METtide; MET2 Ac-ARDMYDKEYYSVHN-K). The C-terminal cMet peptide (Ac-ARDMYDKEYYSVHNK) was synthesized (Pfizer, La Jolla) to >90% purity.

Expression and Purification of Proteins. The expression and purification of the VEGFR2 proteins encompassing the catalytic domain (VEGFR2-CD) and the catalytic domain with the juxtamembrane domain (VEGFR2-CD/JM) have been described.[10] Two codon optimized (Geneart) human VEGFR2 genes comprising the catalytic and juxtamembrane domains (residues 786−1171, VEGFR2-CD/JM) and the catalytic domain (residues 806−1171, VEGFR2-CD) without the kinase insert domain deletions (residues 940−989) containing one point mutation (E990V) were cloned into pFastBac vectors. The VEGFR2-CD/JM protein had an N-terminal His$_6$ tag followed by an HRV3C protease cleavage site, and the VEGFR2-CD contained a C-terminal His$_6$ tag with an upstream TEV protease site. Proteins were expressed in *Sf9* cells and harvested 48 h post infection. Clarified cell lysate was purified using a Probond Nickel column (Invitrogen). Tag removal achieved with protease treatment and overnight dialysis. Nickel chromatography removed uncleaved protein and free His$_6$ tag. Untagged proteins were purified by HiLoad 26/60 Superdex-75 (GE Healthcare) gel filtration (50 mM HEPES 7.5, 30 mM NaCl, 5 mM DTT), concentrated to 8−13 mg mL^{-1}, flash-frozen in liquid nitrogen, and stored at −80 °C. VEGFR2-CD and VEGFR2-CD/JM proteins were determined to be not phosphorylated by intact mass spectrometry. Autophosphorylation procedures have been previously published.[10] FGFR-1 catalytic domain (aa 456−765) and VEGFR1 catalytic domain (aa 827−1158) were purified by a similar procedure as VEGFR2 except the His$_6$-tag was N-terminal prior to cleavage. PDGFRβ was produced as a GST-fusion protein of PDGFRβ (aa 558−1090) and purified with glutathione affinity chromatography. GST-VEGFR2 cytoplasmic domain [790−1356 residues of accession number NP_002244.1] was expressed as N-terminal GST-fusion protein (90 kDa) using baculovirus expression system by Carna Biosciences. GST-KDR was purified by using glutathione sepharose chromatography to 93% purity assessed by SDS-PAGE with an uncharacterized phosphorylation state.

Enzymatic Assays. The spectrophotometric coupled enzymatic assay used to measure VEGFR2 enzymatic activity has been described.[10] The kinase-catalyzed production of ADP is coupled to the oxidation of NADH (340 nm, ε = 6220 cm^{-1} M^{-1}) through the activities of pyruvate kinase (PK) and lactate dehydrogenase (LDH). Typical reaction solutions contained 2 mM phosphoenolpyruvate, 0.33 mM NADH, 50 mM MgCl$_2$, 5 mM DTT, ATP, minigastrin or poly(Glu$_4$Tyr), 15 units mL^{-1} PK, 15 units mL^{-1} LDH in 200 mM HEPES, pH 7.5 at 37 °C. For catalytic parameter determination, ATP was varied from 7.8 to 8000 μM, poly(Glu$_4$Tyr) was varied from 0.013 to 13.7 mg mL^{-1} (20 mM), and minigastrin was varied from 8.3 to 2150 μM. When poly(Glu$_4$Tyr) was used, assays were initiated with the addition of 10 nM nonphosphorylated VEGFR2-CD or VEGFR2-CD/JM; 5 nM nonphosphorylated VEGFR2-CD or VEGFR2-CD/JM when the phosphoacceptor was minigastrin. Kinetic analyses of phosphoacceptors were performed at 3 mM ATP. The K_i determinations were made with a final concentration of 10.8 mM ATP, and poly(Glu$_4$Tyr) was 20 mM. K_i determinations were made from a plot of the fractional velocity as a function of inhibitor concentration fit to the Morrison equation for competitive inhibition with the enzyme concentration as a variable.[10,20,21] VEGFR1 assays were similar except for the following: 40 nM VEGFR1, 3 mM ATP, 40 mM MgCl$_2$, 20 mM poly(Glu$_4$Tyr). FGFR1 assays were similar except for the following: 124 nM FGFR1, 3 mM ATP, 60 mM MgCl$_2$, 15 mM poly(Glu$_4$Tyr). PDGFRβ assays were similar except for the following: 76 nM PDGFRβ, 2 mM ATP, 60 mM MgCl$_2$, 15 mM poly(Glu$_4$Tyr). The $K_{m,ATP}$ values for the kinase catalytic domains are as follows: 2.0 mM (VEGFR1) and 0.341 mM (PDGFRβ). The phosphopeptide products of kinase-mediated peptide reactions were evaluated by mass spectrometry to ensure a single phosphorylation event occurs on each peptide.

Inhibitors were tested in a GST-VEGFR2 assay by Carna Biosciences with the Caliper LabChip3000 assay (Caliper Life Science), which is a mobility-shift assay (MSA) that combines the basic principles of capillary electrophoresis in a microfluidic environment. Compounds were prepared in 100% DMSO, diluted to 25% DMSO with 20 mM HEPES pH 7.5, and added to the reaction for a final DMSO concentration of 6%. Inhibitor concentrations varied from 1.0 to 0.00003 μM. Twenty microliter reactions contained 120 ng mL^{-1} (1.24 nM) KDR, 75 uM ATP ($K_{m,ATP}$ = 74 μM), 1.0 uM CSKtide (5FAM-KKKKEEIYFFF), 5 mM MgCl$_2$, 2 mM DTT, 0.01% Triton X-100, 6.25% DMSO in 20 mM HEPES pH 7.5. The mixture was incubated in a 384-well polypropylene plate at RT for 1 h and terminated by the addition of 60 μL of QuickScout Screening Assist MSA Buffer (Carna Biosciences). The reaction mixture was applied to a LabChip3000 system, and the product/substrate peptide peaks were separated. The kinase reaction was quantitated by the product ratio calculated from peak heights of product (P) and substrate (S) peptides ($P/(P + S)$). IC$_{50}$ values were transformed to K_i value using the Cheng−Prusoff equation.

VEGF-Induced Cellular Assays. The VEGF-induced VEGFR-2 autophosphorylation assay in porcine aorta endothelial (PAE) cells overexpressing full-length VEGFR-2 has been previously described.[22,23] PAE-KDR cells were seeded at 25,000 cells/well in 96-well plates in F-12 (Ham) plus 10% FBS and G418 overnight. The cells were then serum starved in F-12 plus 0.1% FBS and 0.2% BSA for 20 h. The cells were treated with compounds formulated in 0.1% DMSO in the starvation medium at 1:3 serial dilution in duplicates for 1 h at 37 °C plus CO$_2$ and stimulated with 50 ng mL^{-1} rhVEGF (R&D Systems) for 5 min. The positive control cells received VEGF only without compounds, and the negative control cells received starvation medium only without VEGF or compounds. Cells were lysed in 100 μL/well in cell lysis buffer (Cell Signaling) for 25 min (at 4 °C) with lysate transferred to pVEGFR2 ELISA plate (Cell Signaling) and measured with the manufacture's protocol (Cell Signaling, Beverly, MA) at 450 nm on EnVision plate reader (Perkin-Elmer).

The VEGF-dependent cell survival assay in human umbilical vein endothelial cells (HUVEC) has been previously described.[10] HUVEC (passage <5, Lonza) were plated in 100 μL of F12K growth medium at a concentration of 1 × 10^4 cells per well in a 96-well plate overnight. Cells were then starved in 1% FBS F12K media for 24 h. Compounds formulated in 0.3% DMSO in the starvation medium were added in triplicate to obtain a dose response curve (1:3 dilution). One hour after compound treatment, cells were stimulated with rhVEGF (R&D systems) at a final concentration of 25 ng mL^{-1}. After 72 h of incubation, HUVEC survival was measured via Resazurin fluorescent assay (Promega) with fluorescence at 530 nm/590 nm. IC$_{50}$ values were calculated using negative (no rhVEGF, no compound) and positive (rhVEGF, no compound) controls as 0% and 100% survival, respectively.

■ AUTHOR INFORMATION

Corresponding Author
*E-mail: brion.murray@pfizer.com.

Notes
The authors declare no competing financial interests.

REFERENCES

(1) Schwartz, P. A., and Murray, B. W. (2011) Protein kinase biochemistry and drug discovery. Bioorg. Chem. 39, 192−210.

(2) Folkman, J. (2007) Angiogenesis: an organizing principle for drug discovery? Nat. Rev. Drug Discovery 6, 273−286.

(3) Manning, G., Whyte, D. B., Martinez, R., Hunter, T., and Sudarsanam, S. (2002) The protein kinase complement of the human genome. Science 298, 1912−1934.

(4) Kowanetz, M., and Ferrara, N. (2006) Vascular endothelial growth factor signaling pathways: therapeutic perspective. Clin. Cancer Res. 12, 5018−5022.

(5) Olsson, A. K., Dimberg, A., Kreuger, J., and Claesson-Welsh, L. (2006) VEGF receptor signalling − in control of vascular function. Nat. Rev. Mol. Cell. Biol. 7, 359−371.

(6) Takahashi, T., and Shibuya, M. (1997) The 230 kDa mature form of KDR/Flk-1 (VEGF receptor-2) activates the PLC-gamma pathway and partially induces mitotic signals in NIH3T3 fibroblasts. Oncogene 14, 2079−2089.

(7) McTigue, M. A., Wickersham, J. A., Pinko, C., Showalter, R. E., Parast, C. V., Tempczyk-Russell, A., Gehring, M. R., Mroczkowski, B., Kan, C. C., Villafranca, J. E., and Appelt, K. (1999) Crystal structure of the kinase domain of human vascular endothelial growth factor receptor 2: a key enzyme in angiogenesis. Structure 7, 319−330.

(8) Roskoski, R., Jr. (2008) VEGF receptor protein-tyrosine kinases: structure and regulation. Biochem. Biophys. Res. Commun. 375, 287−291.

(9) Eichmann, A., and Simons, M. (2012) VEGF signaling inside vascular endothelial cells and beyond. Curr. Opin. Cell Biol. 24, 188−193.

(10) Solowiej, J., Bergqvist, S., McTigue, M. A., Marrone, T., Quenzer, T., Cobbs, M., Ryan, K., Kania, R. S., Diehl, W., and Murray, B. W. (2009) Characterizing the effects of the juxtamembrane domain on vascular endothelial growth factor receptor-2 enzymatic activity, autophosphorylation, and inhibition by axitinib. Biochemistry 48, 7019−7031.

(11) Dougher-Vermazen, M., Hulmes, J. D., Bohlen, P., and Terman, B. I. (1994) Biological activity and phosphorylation sites of the bacterially expressed cytosolic domain of the KDR VEGF-receptor. Biochem. Biophys. Res. Commun. 205, 728−738.

(12) Takahashi, T., Yamaguchi, S., Chida, K., and Shibuya, M. (2001) A single autophosphorylation site on KDR/Flk-1 is essential for VEGF-A-dependent activation of PLC-gamma and DNA synthesis in vascular endothelial cells. EMBO J. 20, 2768−2778.

(13) Dayanir, V., Meyer, R. D., Lashkari, K., and Rahimi, N. (2001) Identification of tyrosine residues in vascular endothelial growth factor receptor-2/FLK-1 involved in activation of phosphatidylinositol 3-kinase and cell proliferation. J. Biol. Chem. 276, 17686−17692.

(14) Meyer, R. D., Dayanir, V., Majnoun, F., and Rahimi, N. (2002) The presence of a single tyrosine residue at the carboxyl domain of vascular endothelial growth factor receptor-2/FLK-1 regulates its autophosphorylation and activation of signaling molecules. J. Biol. Chem. 277, 27081−27087.

(15) Sakurai, Y., Ohgimoto, K., Kataoka, Y., Yoshida, N., and Shibuya, M. (2005) Essential role of Flk-1 (VEGF receptor 2) tyrosine residue 1173 in vasculogenesis in mice. Proc. Natl. Acad. Sci. U.S.A. 102, 1076−1081.

(16) McTigue, M., Murray, B. W., Chen, J. H., Deng, Y. L., Solowiej, J., and Kania, R. S. (2012) Feature Article: Molecular conformations, interactions, and properties associated with drug efficiency and clinical performance among VEGFR TK inhibitors. Proc. Natl. Acad. Sci. U.S.A. 109, 18281−18289.

(17) Bruns, A. F., Herbert, S. P., Odell, A. F., Jopling, H. M., Hooper, N. M., Zachary, I. C., Walker, J. H., and Ponnambalam, S. (2010) Ligand-stimulated VEGFR2 signaling is regulated by co-ordinated trafficking and proteolysis. Traffic 11, 161−174.

(18) Zuccotto, F., Ardini, E., Casale, E., and Angiolini, M. (2010) Through the ″gatekeeper door″: exploiting the active kinase conformation. J. Med. Chem. 53, 2681−2694.

(19) Ellis, L. M., and Hicklin, D. J. (2008) VEGF-targeted therapy: mechanisms of anti-tumour activity. Nat. Rev. Cancer. 8, 579−591.

(20) Morrison, J. F. (1969) Kinetics of the reversible inhibition of enzyme-catalysed reactions by tight-binding inhibitors. Biochim. Biophys. Acta 185, 269−286.

(21) Murphy, D. J. (2004) Determination of accurate KI values for tight-binding enzyme inhibitors: an in silico study of experimental error and assay design. Anal. Biochem. 327, 61−67.

(22) Waltenberger, J., Claesson-Welsh, L., Siegbahn, A., Shibuya, M., and Heldin, C. H. (1994) Different signal transduction properties of KDR and Flt1, two receptors for vascular endothelial growth factor. J. Biol. Chem. 269, 26988−26995.

(23) Hu-Lowe, D. D., Zou, H. Y., Grazzini, M. L., Hallin, M. E., Wickman, G. R., Amundson, K., Chen, J. H., Rewolinski, D. A., Yamazaki, S., Wu, E. Y., McTigue, M. A., Murray, B. W., Kania, R. S., O'Connor, P., Shalinsky, D. R., and Bender, S. L. (2008) Nonclinical antiangiogenesis and antitumor activities of axitinib (AG-013736), an oral, potent, and selective inhibitor of vascular endothelial growth factor receptor tyrosine kinases 1, 2, 3. Clin. Cancer Res. 14, 7272−7283.

(24) Kania, R. (2009) Structure Based Design and Characterization of Axitinib, in Kinase Inhibitor Drugs (Li, R. and Stafford, J. A., Eds.), pp 167−201, John Wiley and Sons, Hoboken, NJ.

(25) Zhang, J., Yang, P. L., and Gray, N. S. (2009) Targeting cancer with small molecule kinase inhibitors. Nat. Rev. Cancer. 9, 28−39.

(26) Goldsmith, E. J., Akella, R., Min, X., Zhou, T., and Humphreys, J. M. (2007) Substrate and docking interactions in serine/threonine protein kinases. Chem. Rev. 107, 5065−5081.

(27) Kornev, A. P., and Taylor, S. S. (2010) Defining the conserved internal architecture of a protein kinase. Biochim. Biophys. Acta 1804, 440−444.

(28) Grabowska, A. M., and Watson, S. A. (2007) Role of gastrin peptides in carcinogenesis. Cancer Lett. 257, 1−15.

(29) Burkitt, M. D., Varro, A., and Pritchard, D. M. (2009) Importance of gastrin in the pathogenesis and treatment of gastric tumors. World J. Gastroenterol. 15, 1−16.

(30) Ferrand, A., and Wang, T. C. (2006) Gastrin and cancer: a review. Cancer Lett. 238, 15−29.

(31) Mathieu, V., Mijatovic, T., van Damme, M., and Kiss, R. (2005) Gastrin exerts pleiotropic effects on human melanoma cell biology. Neoplasia 7, 930−943.

(32) Watson, S. A., Grabowska, A. M., El-Zaatari, M., and Takhar, A. (2006) Gastrin - active participant or bystander in gastric carcinogenesis? Nat. Rev. Cancer 6, 936−946.

(33) Baldwin, G. S., Knesel, J., and Monckton, J. M. (1983) Phosphorylation of gastrin-17 by epidermal growth factor-stimulated tyrosine kinase. Nature 301, 435−437.

(34) Polverino, A., Coxon, A., Starnes, C., Diaz, Z., DeMelfi, T., Wang, L., Bready, J., Estrada, J., Cattley, R., Kaufman, S., Chen, D., Gan, Y., Kumar, G., Meyer, J., Neervannan, S., Alva, G., Talvenheimo, J., Montestruque, S., Tasker, A., Patel, V., Radinsky, R., and Kendall, R. (2006) AMG 706, an oral, multikinase inhibitor that selectively targets vascular endothelial growth factor, platelet-derived growth factor, and kit receptors, potently inhibits angiogenesis and induces regression in tumor xenografts. Cancer Res. 66, 8715−8721.

(35) Norman, M. H., Liu, L., Lee, M., Xi, N., Fellows, I., D'Angelo, N. D., Dominguez, C., Rex, K., Bellon, S. F., Kim, T. S., and Dussault, I. (2012) Structure-based design of novel class II c-Met inhibitors: 1. Identification of pyrazolone-based derivatives. J. Med. Chem. 55, 1858−1867.

(36) Liu, L., Norman, M. H., Lee, M., Xi, N., Siegmund, A., Boezio, A. A., Booker, S., Choquette, D., D'Angelo, N. D., Germain, J., Yang, K., Yang, Y., Zhang, Y., Bellon, S. F., Whittington, D. A., Harmange, J. C., Dominguez, C., Kim, T. S., and Dussault, I. (2012) Structure-based

design of novel class II c-Met inhibitors: 2. SAR and kinase selectivity profiles of the pyrazolone series. *J. Med. Chem. 55*, 1868−1897.

(37) Frey, P. A., and Hegeman, A. D. (2007) *Enzymatic Reaction Mechanism*, Oxford University Press, New York.

(38) Gajiwala, K. S., Wu, J. C., Christensen, J., Deshmukh, G. D., Diehl, W., DiNitto, J. P., English, J. M., Greig, M. J., He, Y. A., Jacques, S. L., Lunney, E. A., McTigue, M., Molina, D., Quenzer, T., Wells, P. A., Yu, X., Zhang, Y., Zou, A., Emmett, M. R., Marshall, A. G., Zhang, H. M., and Demetri, G. D. (2009) KIT kinase mutants show unique mechanisms of drug resistance to imatinib and sunitinib in gastrointestinal stromal tumor patients. *Proc. Natl. Acad. Sci. U.S.A. 106*, 1542−1547.

(39) Card, A., Caldwell, C., Min, H., Lokchander, B., Hualin, X., Sciabola, S., Kamath, A. V., Clugston, S. L., Tschantz, W. R., Leyu, W., and Moshinsky, D. J. (2009) High-throughput biochemical kinase selectivity assays: panel development and screening applications. *J. Biomol. Screening 14*, 31−42.